

# Exploring the Electronic and Optical Properties of $\text{Cu}(\text{In},\text{Ga})\text{Se}_2$

Rongzhen Chen

Supervisor: Clas Persson

Department of Materials Science and Engineering  
Royal Institute of Technology, Stockholm SE-10044, Sweden

06-March-2015



# Outline

1 Background

2 Motivation

3 Computational methods

4 Results

- Paper 1: parameterization of energy bands for CIGS
- Paper 2: analysis of density-of-states (DOS) and carrier concentration
- Paper 3: dielectric function for  $\text{CuIn}_{0.5}\text{Ga}_{0.5}\text{Se}_2$

5 Summary

6 Future perspectives

7 Acknowledgements

1 Background

2 Motivation

3 Computational methods

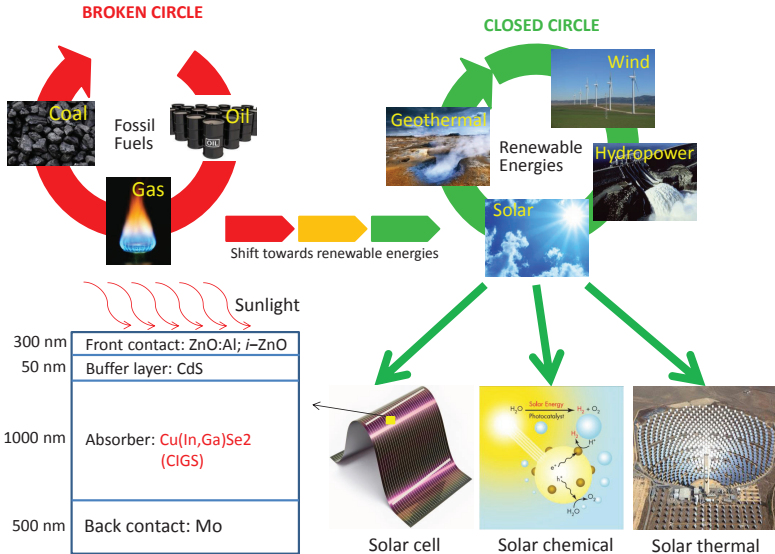
4 Results

5 Summary

6 Future perspectives

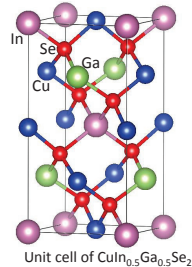
7 Acknowledgements

# Which field and material am I working on?



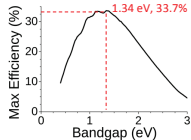
# Why Cu(In,Ga)Se<sub>2</sub>?

CIS = CuInSe<sub>2</sub>  
CGS = CuGaSe<sub>2</sub>  
CIGS = Cu(In, Ga)Se<sub>2</sub> = CuIn<sub>1-x</sub>Ga<sub>x</sub>Se<sub>2</sub>



Advantages of CIGS:

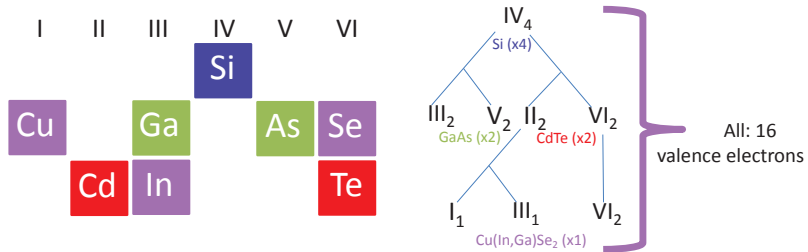
1. Tunable band-gap (1.0 to 1.7 eV)
2. Efficiency 23.3% in the lab
3. High absorption coefficient, thinner, flexible



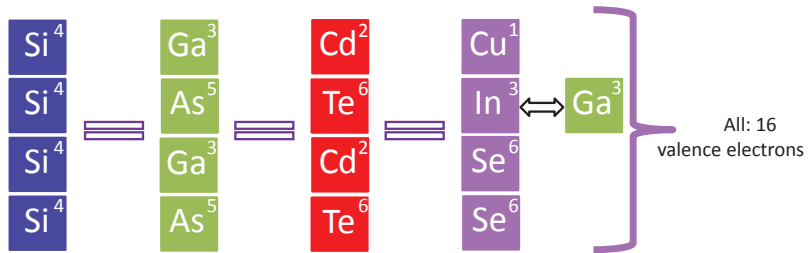
The Shockley-Queisser limit for the efficiency of a solar cell.

CIGS is doing well in the Building-integrated photovoltaics market.

# Where does Cu(In,Ga)Se<sub>2</sub> come from?



A series of cation mutations where total number of valence electrons is the same and it keeps the charge neutral in the compound.



1 Background

2 Motivation

3 Computational methods

4 Results

5 Summary

6 Future perspectives

7 Acknowledgements

# Which aspects of Cu(In,Ga)Se<sub>2</sub> have I been working on?

- Electronic structure

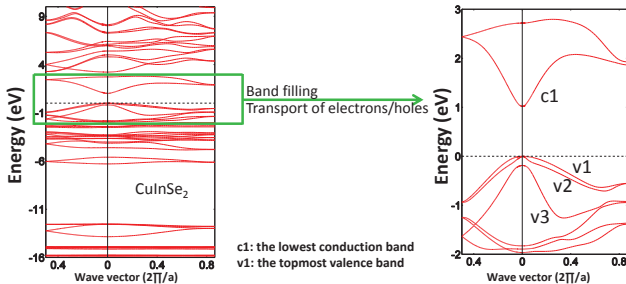
- Energy bands of CuInSe<sub>2</sub>, CuIn<sub>0.5</sub>Ga<sub>0.5</sub>Se<sub>2</sub>, and CuGaSe<sub>2</sub> are calculated by means of theoretical calculations. Parameterization of the lowest conduction (CB) and the three uppermost valence bands (VBs) are explored based on the calculated energy bands.
- Analysis of density-of-states (DOS) and carrier concentration based on the parameterization.

- Optical properties

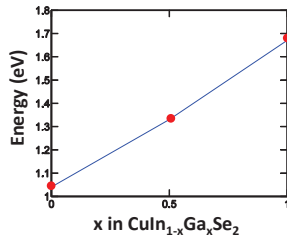
- Dielectric function of CuIn<sub>0.5</sub>Ga<sub>0.5</sub>Se<sub>2</sub> are explored by means of theoretical calculations. The band-to-band optical transitions are analyzed. The electronic origins of the observed interband critical points of the optical response are discussed.

# Motivation for the parameterization

By understanding the electronic properties one can understand many of the fundamental material properties.



1. Less study on CuIn<sub>0.5</sub>Ga<sub>0.5</sub>Se<sub>2</sub>.
2. Commercially interesting: CuIn<sub>0.7</sub>Ga<sub>0.3</sub>Se<sub>2</sub>, CuIn<sub>0.5</sub>Ga<sub>0.5</sub>Se<sub>2</sub> indicates how CIGS behaves when alloying In and Ga.



# Motivation for analysis of DOS and carrier concentration

- Better analyze the impact on DOS as well as carrier concentration taking into account the non-parabolicity of the energy bands.
- Help experimentalists to reproduce DOS from energy-dependent DOS mass.
- DOS and carrier concentration obtained by full band parameterization and parabolic band approximation are compared.

# Motivation for calculation of dielectric function

Absorption coefficient can be calculated by dielectric function directly, and thickness of material is determined by the absorption coefficient.

- Help experimentalists to understand the dielectric function spectrum.
- Understand details in the optical transition for these types of materials.

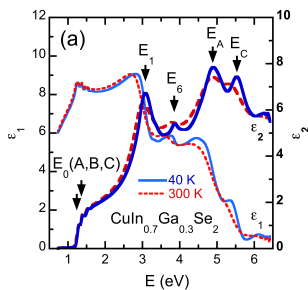


Figure : The real ( $\epsilon_1$ ) and imaginary ( $\epsilon_2$ ) part of dielectric function spectra.

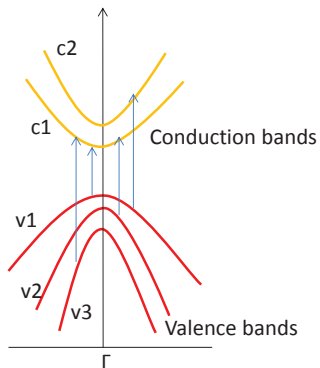


Figure : Energy bands.

- 1 Background
- 2 Motivation
- 3 Computational methods
- 4 Results
- 5 Summary
- 6 Future perspectives
- 7 Acknowledgements

# Density functional theory (DFT)

DFT-based modeling is extremely successful in many-body systems.

- DFT was introduced by Hohenberg and Kohn in 1964. Kohn and Pople were awarded Chemistry Nobel Prize in 1998.
- Around 20,000 papers per year.

DFT says that ground-state total energy ( $E_{total}[\rho]$ ) can be determined from the ground-state charge density  $\rho$  instead of many-electron wavefunction. However, we do not have explicit form for  $E_{total}[\rho]$ .

# Kohn-Sham (KS) Equation

This problem in DFT is solved by KS equation:

$$E_{total}[\rho] = T_0[\rho] + V_H[\rho] + V_{ext}[\rho] + E_{xc}[\rho]. \quad (1)$$

The KS equation is derived as

$$\left( -\frac{\nabla^2}{2} + V^{KS}(\mathbf{r}) \right) \Psi_i^{KS}(\mathbf{r}) = \epsilon_i^{KS} \Psi_i^{KS}(\mathbf{r}). \quad (2)$$

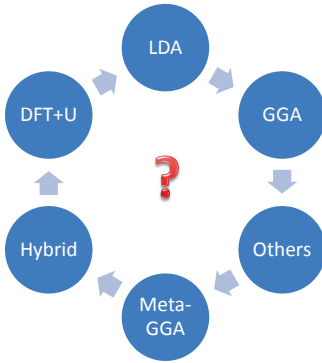
The  $V^{KS}(\mathbf{r})$  is given as

$$V^{KS}(\mathbf{r}) = V_{ext}(\mathbf{r}) + \int d\mathbf{r}' \frac{\rho(\mathbf{r}')}{|\mathbf{r} - \mathbf{r}'|} + \overbrace{\frac{\delta E_{xc}}{\delta \rho(\mathbf{r})}}^{V_{xc}(\mathbf{r})}. \quad (3)$$

Here

$$\rho = \sum |\Psi_i^{KS}(\mathbf{r})|^2. \quad (4)$$

# Different exchange-correlation potentials $V_{xc}(\mathbf{r})$



In our calculations, we took the GGA+U (d-states), which was proved to improve the effective mass, that is curvature of energy band. ???? explain LDA GGA ....

1 Background

2 Motivation

3 Computational methods

4 Results

- Paper 1: parameterization of energy bands for CIGS
- Paper 2: analysis of density-of-states (DOS) and carrier concentration
- Paper 3: dielectric function for  $\text{CuIn}_{0.5}\text{Ga}_{0.5}\text{Se}_2$

5 Summary

6 Future perspectives

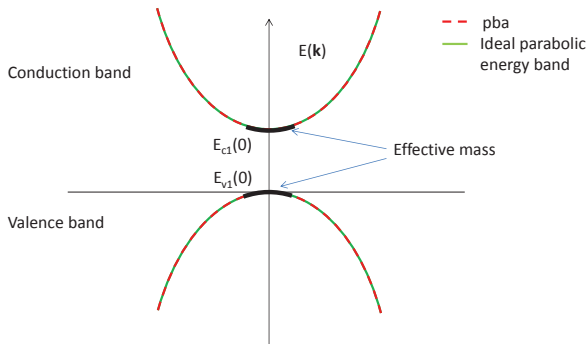
7 Acknowledgements

# Paper 1: parabolic band approximation (pba)

The parabolic approximation of ellipsoidal energy bands is expressed

$$E_j^{pb}(\mathbf{k}) = E_j(\mathbf{0}) \pm \left[ \frac{\tilde{\mathbf{k}}_x^2 + \tilde{\mathbf{k}}_y^2}{m_j^{xy}} + \frac{\tilde{\mathbf{k}}_z^2}{m_j^z} \right] \quad (5)$$
$$m^{ab} = \pm \hbar^2 / (\partial E(\mathbf{k}) / \partial k_a k_b).$$

In the case of ideal parabolic energy band, the pba can describe energy band perfectly.

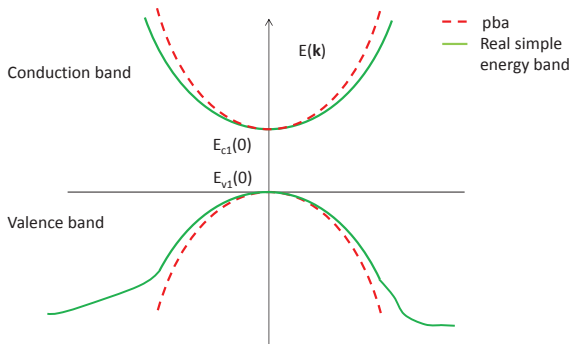


# Paper 1: parabolic band approximation (pba)

The parabolic approximation of ellipsoidal energy bands is expressed

$$E_j^{pb}(\mathbf{k}) = E_j(\mathbf{0}) \pm \left[ \frac{\tilde{\mathbf{k}}_x^2 + \tilde{\mathbf{k}}_y^2}{m_j^{xy}} + \frac{\tilde{\mathbf{k}}_z^2}{m_j^z} \right] \quad (6)$$
$$m^{ab} = \pm \hbar^2 / (\partial E(\mathbf{k}) / \partial k_a k_b).$$

The parabolic approximation is valid in the vicinity of the  $\Gamma$ -point. However, away from the  $\Gamma$ -point, it fails to describe the energy dispersion.

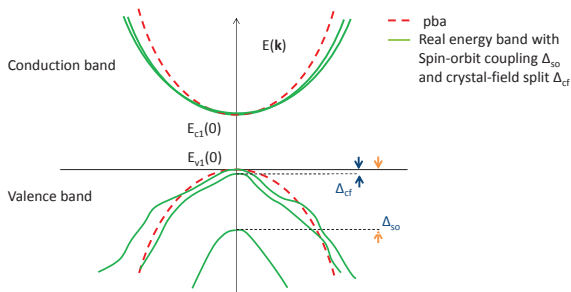


# Paper 1: parabolic band approximation (pba)

The parabolic approximation of ellipsoidal energy bands is expressed

$$E_j^{pb}(\mathbf{k}) = E_j(\mathbf{0}) \pm \left[ \frac{\tilde{\mathbf{k}}_x^2 + \tilde{\mathbf{k}}_y^2}{m_j^{xy}} + \frac{\tilde{\mathbf{k}}_z^2}{m_j^z} \right] \quad (7)$$
$$m^{ab} = \pm \hbar^2 / (\partial E(\mathbf{k}) / \partial k_a k_b).$$

Considering spin-orbit coupling and crystal-field split, the energy band becomes very complicated. The parabolic approximation is valid in the very vicinity of the  $\Gamma$ -point.



# Paper 1: Full band parameterization (fbp)

$$\begin{aligned} E_j(\mathbf{k}) = & E_j^{pb}(\mathbf{k}) + E_j^0 + \Delta_{j,1} \left( \delta_{j,1}^2 \left( \frac{\tilde{\mathbf{k}}_x^4 + \tilde{\mathbf{k}}_y^4}{m_0^2} \right) + \delta_{j,2}^2 \left( \frac{\tilde{\mathbf{k}}_x^2 \tilde{\mathbf{k}}_y^2}{m_0^2} \right) + 1 \right)^{1/2} \\ & + \Delta_{j,2} \left( \delta_{j,3}^3 \left( \frac{\tilde{\mathbf{k}}_x^6 + \tilde{\mathbf{k}}_y^6}{m_0^3} \right) + \delta_{j,4}^3 \left( \frac{\tilde{\mathbf{k}}_x^2 \tilde{\mathbf{k}}_y^4 + \tilde{\mathbf{k}}_x^4 \tilde{\mathbf{k}}_y^2}{m_0^3} \right) + 1 \right)^{1/3} \\ & + \Delta_{j,3} \left( \delta_{j,5}^2 \left( \frac{\tilde{\mathbf{k}}_z^4}{m_0^2} \right) + 1 \right)^{1/2} + \Delta_{j,4} \left( \delta_{j,6}^3 \left( \frac{\tilde{\mathbf{k}}_z^6}{m_0^3} \right) + 1 \right)^{1/3} \\ & + \Delta_{j,5} \left( \delta_{j,7}^2 \left( \frac{\tilde{\mathbf{k}}_x^2 \tilde{\mathbf{k}}_z^2 + \tilde{\mathbf{k}}_y^2 \tilde{\mathbf{k}}_z^2}{m_0^2} \right) + 1 \right)^{1/2} \\ & + \Delta_{j,6} \left( \delta_{j,8}^3 \left( \frac{\tilde{\mathbf{k}}_x^4 \tilde{\mathbf{k}}_z^2 + \tilde{\mathbf{k}}_y^4 \tilde{\mathbf{k}}_z^2}{m_0^3} \right) + \delta_{j,9}^3 \left( \frac{\tilde{\mathbf{k}}_x^2 \tilde{\mathbf{k}}_z^4 + \tilde{\mathbf{k}}_y^2 \tilde{\mathbf{k}}_z^4}{m_0^3} \right) + \delta_{j,10}^3 \left( \frac{\tilde{\mathbf{k}}_x^2 \tilde{\mathbf{k}}_y^2 \tilde{\mathbf{k}}_z^2}{m_0^3} \right) + 1 \right)^{1/3} \end{aligned} \quad (8)$$

# Paper 1: Parameterization of band structure for CIGS

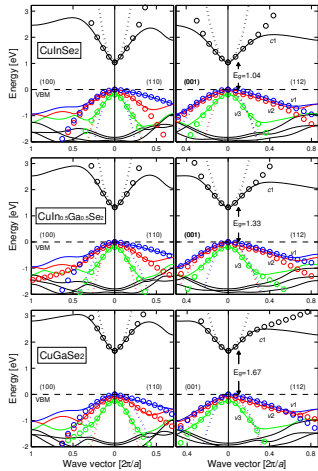


**Figure :** Electronic band structure along four directions. The circles are the results of the fbp, the dotted lines represent the pba, and

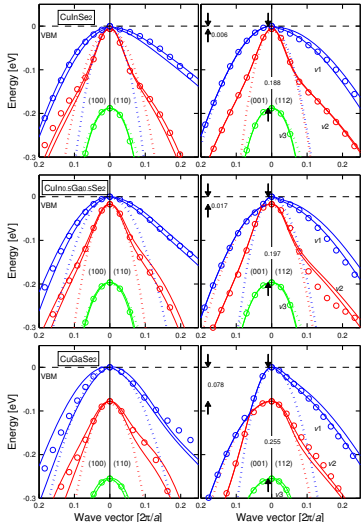


**Figure :** Close-up of the right fig-

# Paper 1: Non-parabolicity of the energy bands

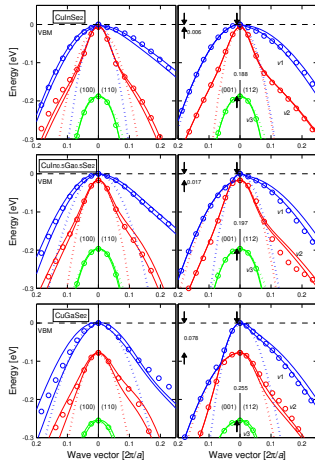


**Figure :** Close-up of electronic band structure. The circles are the results of the fbp, the dotted lines represent the pba, and the solid lines represent the theoretical cal-

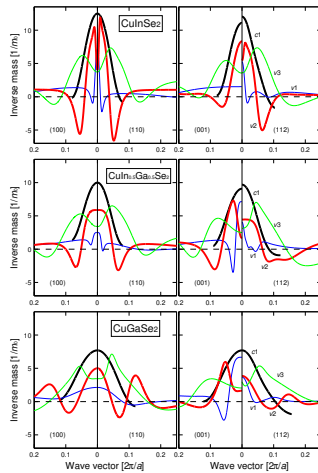


**Figure :** Inverse of the effective electron and hole masses in the four symmetry directions for the  $\text{CuIn}_x\text{Ga}_{1-x}\text{Se}_2$  ( $x = 0, 0.5$ , and  $1$ )

# Paper 1: Non-parabolicity of the energy bands

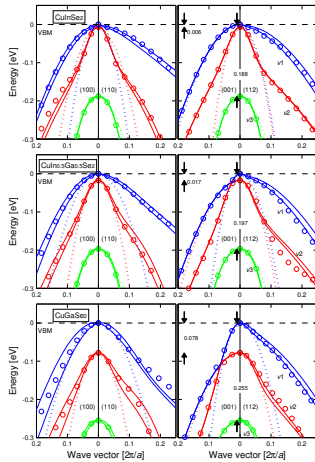


**Figure :** Close-up of electronic band structure. The circles are the results of the fbp, the dotted lines represent the pba, and the solid lines represent the theoretical cal-

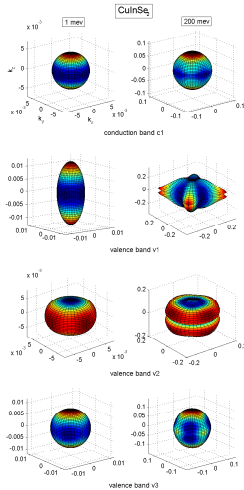


**Figure :** Constant energy surfaces for the lowest CB and three uppermost VBs in CuInSe<sub>2</sub>

## Paper 2: Density-of-states (DOS)

In the case of the pba, the density-of-states can be written as

$$g_j^{pba}(E) = \frac{1}{2\pi^2} \left( \frac{2m_j^{DOS}}{\hbar^2} \right)^{3/2} \sqrt{|E - E_j(\mathbf{0})|}. \quad (9)$$

In order to take advantage of the simple **Eq. 9** for the non-parabolic energy bands, the energy-dependent DOS mass ( $m_{v/c}^{DOS}$ ) is defined as

$$g_{v/c}(E) = \sum_j g_j(E) = \frac{1}{2\pi^2} \left( \frac{2m_{v/c}^{DOS}(E)}{\hbar^2} \right)^{3/2} \sqrt{|E - E_{v1/c1}(\mathbf{0})|}. \quad (10)$$

# Paper 2: Density-of-states (DOS) and DOS mass

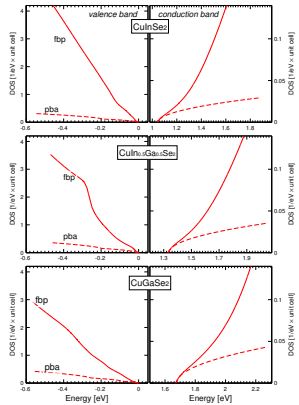


**Figure :** Total DOS of the VBS and CB. The solid lines show the results based on the fbp, and the dashed lines represent the results based on the pba.

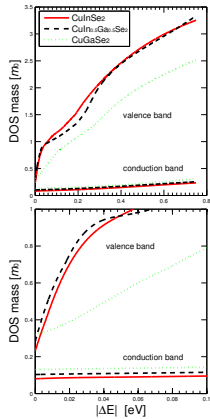


**Figure :** The DOS mass  $m_{v/c}^{DOS}$

## Paper 2: intrinsic carrier concentration

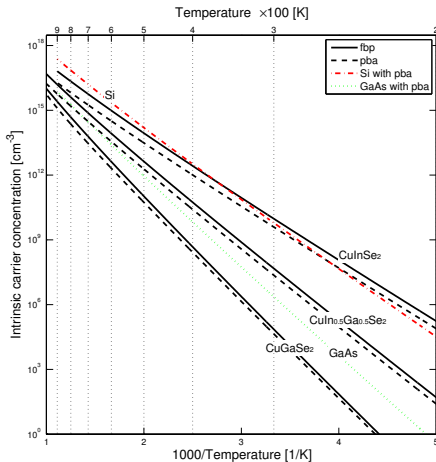


**Figure :** Intrinsic carrier concentration as function of temperature. For comparison, the theoretical results for GaAs and Si using the pba are given.

# Paper 2: Carrier concentration in different temperatures

# Paper 2: Carrier concentration in *p*-type for CIGS

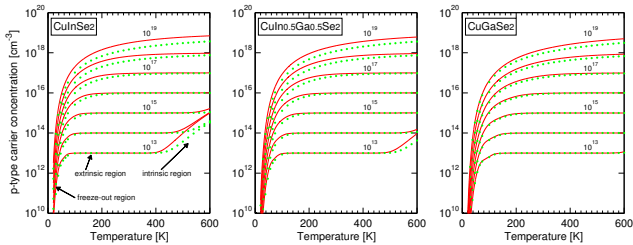


**Figure :** Free carrier concentration as function of the temperature in *p*-type for  $\text{CuInSe}_2$ ,  $\text{CuIn}_{0.5}\text{Ga}_{0.5}\text{Se}_2$ , and  $\text{CuGaSe}_2$ . The effective doping concentration  $N_A = 10^{13}, 10^{14}, 10^{15}, \dots$ , and  $10^{19} \text{ acceptors cm}^{-3}$  are considered. Solid and dotted lines represents the fbp and the pba, respectively.

# Paper 3: Dielectric function for $\text{CuIn}_{0.5}\text{Ga}_{0.5}\text{Se}_2$

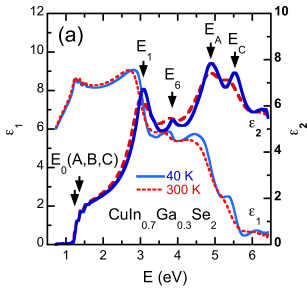


**Figure :** The real ( $\epsilon_1$ ) and imaginary ( $\epsilon_2$ ) part of dielectric function spectra for  $\text{CuIn}_{0.7}\text{Ga}_{0.3}\text{Se}_2$  at 40 K (solid blue line) and 300 K (dashed red lines). Four prominent CP features are shown.

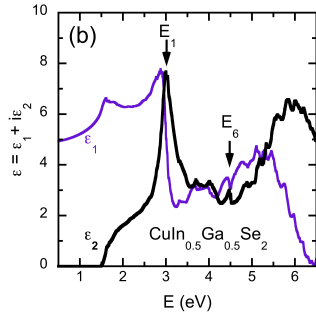


**Figure :** The dielectric function spectra for  $\text{CuIn}_{0.5}\text{Ga}_{0.5}\text{Se}_2$  calculated by FPLAPW method at 0 K. The major CP features are identified.

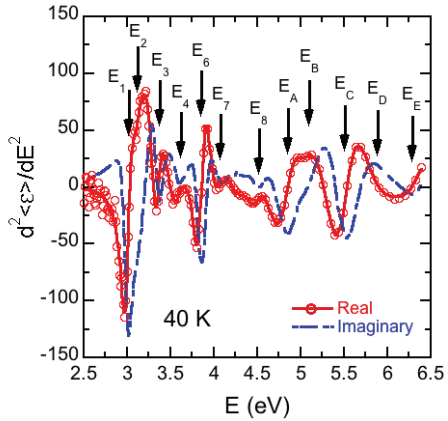
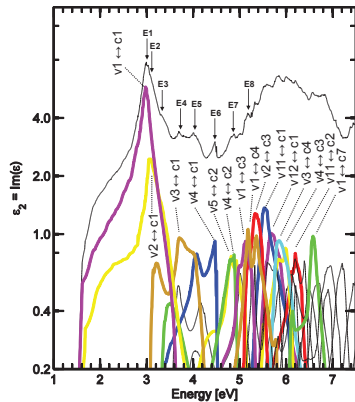
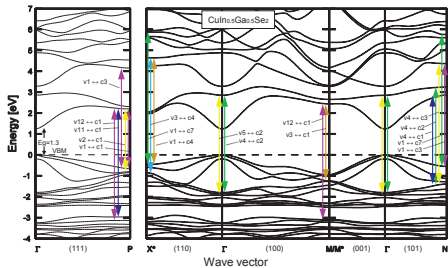


Figure : Energies of each interband critical point (CP) are indicated by arrows and labeled in a numeric and alphabetic order.

# Paper 3: Analysis of the imaginary part of dielectric function



**Figure :** Band-to-band analysis of the contribution to the total  $\epsilon_2$  spectrum. The vertical axis is in the log scale.



**Figure :** The calculated electronic band structure of  $\text{Culn}_{0.5}\text{Ga}_{0.5}\text{Se}_2$  where the CPs are identified along the main symmetry directions.

- 1 Background
- 2 Motivation
- 3 Computational methods
- 4 Results
- 5 Summary
- 6 Future perspectives
- 7 Acknowledgements

# Summary

In this licentiate thesis, two major researches are presented:

- Analysis of the electronic structure of  $\text{CuIn}_{1-x}\text{Ga}_x\text{Se}_2$  with  $x = 0, 0.5$ , and  $1$ . Here, we parameterize the energy bands in order to better describe energy dispersions and better analyze the electron and hole dynamics in the materials. We consider intrinsic and  $p$ -type materials, and we model the temperature dependence.
- Analysis of the optical properties of  $\text{CuIn}_{0.5}\text{Ga}_{0.5}\text{Se}_2$ . Here, the dielectric function spectra is calculated and compared with experimental result. The probable electronic origins of the critical point features are discussed as well.

- 1 Background
- 2 Motivation
- 3 Computational methods
- 4 Results
- 5 Summary
- 6 Future perspectives
- 7 Acknowledgements

# Future perspectives

- The cost and scarcity of indium in the CIGS device is a problem, and copper zinc tin selenide/sulfide (CZT(S,Se)) can therefore be alternative to CIGS due to the low cost and non-toxicity elements.

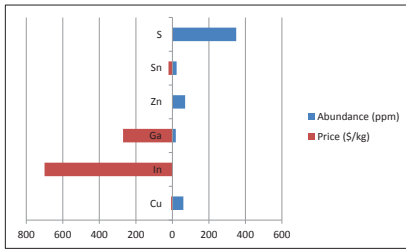


Figure : Abundance and price of Cu, In, Ga, S, Sn, and Zn in Earth's crust (parts per million (ppm) in mass; 10,000 ppm = 1%).

- If there are other similar materials that are of interest. CIGS and CZT(S,Se) can be considered to be in a class denoted as Cu-XY-chalcogenide, where X and Y are two cation elements that replace the group-III In or Ga in CIGS.

- 1 Background
- 2 Motivation
- 3 Computational methods
- 4 Results
- 5 Summary
- 6 Future perspectives
- 7 Acknowledgements

# Acknowledgements

- I would like to express my sincere appreciation to my supervisor Prof. Clas Persson for his academic encouragement and professional guidance.
- I would like to thank all the group colleagues in Stockholm and Oslo for helpful research discussions and chatting. I would like to thank all other people at the Department of Material Sciences and Engineering at KTH for creating a nice working atmosphere.
- The China Scholarship Council, the Swedish Energy Agency, the Swedish Research Council, Stiftelsen Axel Hultgrens fond, Olle Erikssons stiftelse for materialteknik, and KTH Computational Science and Engineering Centre (KCSE) are acknowledged for financial support.

*Thank you for your attention!*

Rongzhen Chen  
[Rongzhen.Chen@mse.kth.se](mailto:Rongzhen.Chen@mse.kth.se)

# Full-potential linearised augmented-plane wave (FPLAPW)

Unit cell is divided into two regions: one is sphere region called muffin tin (MT) region, which is defined by the center of atom, but non-overlap each sphere; the remaining region is called interstitial ( $I$ ) region.

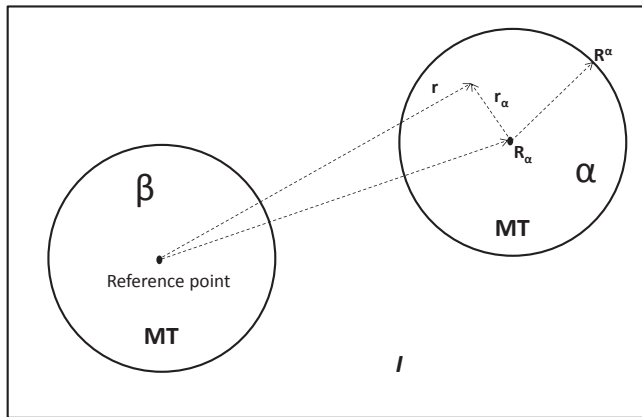


Figure : Partition of the unit cell.

The KS wavefunction can be expanded by a set of basis functions

$$\Psi_{i,\mathbf{k}}^{KS}(\mathbf{r}) = \sum_{\mathbf{G}}^{N_G} C_{i,\mathbf{k}+\mathbf{G}} \phi_{\mathbf{k}+\mathbf{G}}^{LAPW}(\mathbf{r}). \quad (11)$$

Here

$$\phi_{\mathbf{k}+\mathbf{G}}^{LAPW}(\mathbf{r}) = \begin{cases} \frac{1}{\sqrt{\Omega}} e^{i(\mathbf{k}+\mathbf{G})\mathbf{r}} & \text{if } \mathbf{r} \in I \\ \sum_{\alpha} \sum_{\ell m} f_{\ell m}(r_{\alpha}, \mathbf{k} + \mathbf{G}, \epsilon_{\ell, \alpha}) Y_{\ell m}(\hat{\mathbf{r}}_{\alpha}) & \text{if } r_{\alpha} \in MT. \end{cases} \quad (12)$$

The potential in the FPLAPW method is also divided into two regions, the MT region and the  $I$  region.

$$V(\mathbf{r}) = \begin{cases} \sum_{\mathbf{G}} V_{\mathbf{G}} e^{i\mathbf{Gr}} & \text{if } \mathbf{r} \in I \\ \sum_{\ell m} V_{\ell m}^{\alpha}(r_{\alpha}) Y_{\ell m}(\hat{\mathbf{r}}_{\alpha}) & \text{if } r_{\alpha} \in MT. \end{cases} \quad (13)$$

Here,  $V_{\mathbf{G}}$  and  $V_{\ell m}^{\alpha}(r_{\alpha})$  can be decided by electron density.

# The process for solving KS equation

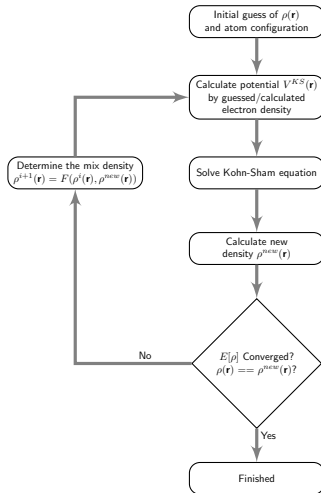
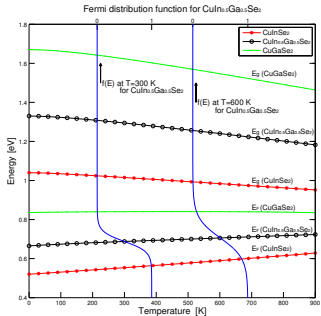
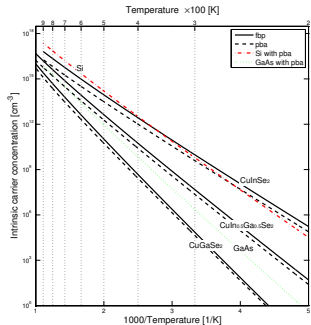


Figure : Flow chart of the  $(i + 1)$ :th iteration for solving KS equation.



**Figure :** Band-gap energy and Fermi energy for  $1 \leq T \leq 900\text{ K}$  of intrinsic  $\text{CuInSe}_2$ ,  $\text{CuIn}_{0.5}\text{Ga}_{0.5}\text{Se}_2$ , and  $\text{CuGaSe}_2$ , determined from the fbp. The Fermi distribution  $f(E)$  of  $\text{CuIn}_{0.5}\text{Ga}_{0.5}\text{Se}_2$  is presented for  $T = 300\text{ K}$  and  $600\text{ K}$ .



**Figure :** Intrinsic carrier concentration as function of temperature. For comparison, the theoretical results for GaAs and Si using the pba are given.

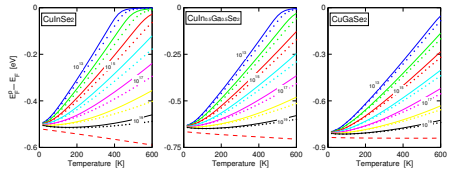


**Figure :** Fermi level as function of the temperature  $20 \leq T \leq 600$  of *p*-type  $\text{CuInSe}_2$ ,  $\text{CuIn}_{0.5}\text{Ga}_{0.5}\text{Se}_2$ , and  $\text{CuGaSe}_2$  for the effective doping concentration  $N_A = 10^{13}$ ,  $10^{14}$ ,  $10^{15}$ , ., and  $10^{19}$  acceptors  $\text{cm}^{-3}$ . Dashed lines represent the VBM with respect to the intrinsic Fermi level. Solid and dotted lines represents the fbp and the pba, respectively.

